

# The evolution of the transverse-momentum dependent gluon distribution at small $x$

Paul Caucal<sup>1,\*</sup> and Edmond Iancu<sup>2,†</sup>

<sup>1</sup>*SUBATECH UMR 6457 (IMT Atlantique, Université de Nantes, IN2P3/CNRS), 4 rue Alfred Kastler, 44307 Nantes, France*

<sup>2</sup>*Université Paris-Saclay, CNRS, CEA, Institut de physique théorique, F-91191, Gif-sur-Yvette, France*

Using the colour dipole picture for photon-nucleus interactions at small  $x$  together with the Color Glass Condensate (CGC) effective theory, we demonstrate that the next-to-leading (NLO) order corrections to the cross-section for the inclusive production of a pair of hard jets encode not only the JIMWLK evolution with decreasing  $x$ , but also the DGLAP evolution of the gluon distribution function and the CSS evolution of the gluon transverse momentum dependent (TMD) distribution. The emergent CSS equation takes the form of a rate equation describing the evolution of the dijet distribution in the transverse momentum imbalance  $K_\perp$  when increasing the dijet relative momentum  $P_\perp$ . All three types of evolution become important when both  $P_\perp$  and  $K_\perp$  are much larger than the nuclear saturation momentum  $Q_s(x)$  and we propose a framework which encompasses all of them. The solution to the JIMWLK equation provides the source term for the DGLAP evolution with increasing  $K_\perp$ , which in turn generates the initial condition for the CSS evolution with increasing  $P_\perp$ .

One of the main challenges in QCD at high energy consists in building a theoretical framework allowing for a simultaneous resummation of small- $x$ , DGLAP and Sudakov logarithms in initial-state parton distribution functions (PDF) [1–10]. In this letter, through the example of inclusive back-to-back dijet production in deep inelastic scattering (DIS), we demonstrate that the TMD factorisation [11, 12] at small  $x$ , as established via explicit calculations [13–35] within the CGC effective theory [36–39], is a natural framework to achieve this goal. The relevant DGLAP logarithms refer to the transverse momentum scales characterising the final state, which are widely separated. This separation introduces new hierarchies in the problem and allows for an additional type of quantum evolution besides the high energy one. Formulated for the gluon TMD, this new evolution encompasses both the Dokshitzer-Gribov-Lipatov-Altarelli-Parisi (DGLAP) [40–42] evolution of the gluon PDF and the Collins-Soper-Sterman (CSS) evolution of the gluon TMD [11, 43–45].

To establish a benchmark for the subsequent discussion of NLO corrections, we first present the leading order (LO) result for the production of a hard quark-antiquark ( $q\bar{q}$ ) pair in high-energy photon-nucleus interactions [13, 14]. The relative transverse momentum  $\mathbf{P} = z_2\mathbf{k}_1 - z_1\mathbf{k}_2$  of the pair is much larger than both its momentum imbalance  $\mathbf{K} = \mathbf{k}_1 + \mathbf{k}_2$  and the target saturation momentum  $Q_s$ . Here  $\mathbf{k}_1$  and  $\mathbf{k}_2$  are the transverse momenta of the quark and the antiquark, and  $z_1 \equiv k_1^+/q^+$  and  $z_2 \equiv k_2^+/q^+ = 1 - z_1$  are their fractions w.r.t. the longitudinal momentum  $q^+$  of the parent photon [46]. We compute this process in the colour dipole picture [47–50], where the  $q\bar{q}$  pair is first generated via the decay of the virtual photon and then is put on-shell by its scattering with the nuclear target. This scattering is most conveniently treated in the transverse coordinate representation, where the  $q\bar{q}$  pair appears as a colour dipole with transverse size  $\mathbf{r} = \mathbf{x} - \mathbf{y}$  and impact pa-

rameter  $\mathbf{b} = z_1\mathbf{x} + z_2\mathbf{y}$  ( $\mathbf{x}$  and  $\mathbf{y}$  are the transverse coordinate of  $q$  and  $\bar{q}$ ). Since this dipole is relatively small,  $r \sim 1/P_\perp \ll 1/Q_s$ , its scattering is weak, yet saturation effects may influence the distribution of the produced particles in the imbalance  $K_\perp$  (which might be as low as  $Q_s$ ) — hence, in the relative azimuthal angle [13, 51, 52].

Multiple scattering in the eikonal approximation can be resummed to all orders within Wilson lines  $V_x, V_y^\dagger$  describing the colour precession of the two fermions. The scattering amplitude reads  $V_x V_y^\dagger - 1 \simeq -r^j V_b \partial^j V_b^\dagger$  to leading order in  $rQ_s \sim Q_s/P_\perp$ . The operator  $\mathcal{A}^i \equiv (i/g)V_b \partial^i V_b^\dagger$  is recognised as the colour field of the target in the *target* light-cone gauge  $\mathcal{A}^- = 0$ .

The light-cone wavefunction (LCWF) describing the  $q\bar{q}$  fluctuation in transverse momentum space is obtained after a Fourier transform [53],

$$\Psi_{\lambda_1\lambda_2}^i(\mathbf{P}, \mathbf{K}, z_1) = -i\sqrt{\frac{q^+}{2}} \frac{ee_f}{(2\pi)^3} \delta_{\lambda_1\lambda_2} \varphi^{il}(z_1, \lambda_1) \times \mathcal{H}^{lj}(\mathbf{P}, z_1) \int d^2\mathbf{b} e^{-i\mathbf{K}\cdot\mathbf{b}} (V_b \partial^j V_b^\dagger), \quad (1)$$

for the case of a transverse photon:  $i$  is the photon polarisation index,  $\lambda_{1,2}$  are spin indices for the two fermions,  $ee_f$  is the electric charge for a quark of flavour  $f$ . The first tensorial factor  $\varphi^{il}(z, \lambda) \equiv (2z - 1)\delta^{il} + 2i\lambda\varepsilon^{il}$  encodes the helicity structure of the photon decay vertex, while the second one (with  $\bar{Q}^2 \equiv z_1 z_2 Q^2$ ),

$$\mathcal{H}^{lj}(\mathbf{P}, z_1) \equiv \frac{1}{P_\perp^2 + \bar{Q}^2} \left( \delta^{lj} - \frac{2P^l P^j}{P_\perp^2 + \bar{Q}^2} \right) \quad (2)$$

describes the  $P_\perp$ -distribution of the  $q\bar{q}$  pair, as generated by the photon decay. The final factor in Eq. (1) (the Fourier transform of the target field) makes it clear that the imbalance  $\mathbf{K}$  is controlled by the scattering.

The factorised structure of the LCWF Eq. (1) transmits

to the LO dijet cross-section, which reads [13, 14]

$$\frac{d\sigma_{\text{LO}}^{\gamma^* A \rightarrow q\bar{q}X}}{dz_1 dz_2 d^2\mathbf{P} d^2\mathbf{K}} = \alpha_{em}\alpha_s e_f^2 \delta(1 - z_1 - z_2) (z_1^2 + z_2^2) \times \frac{P_\perp^4 + \bar{Q}^4}{(P_\perp^2 + \bar{Q}^2)^4} \mathcal{F}_g(x_{q\bar{q}}, K_\perp^2), \quad (3)$$

where the *Weiszäcker-Williams (WW) gluon TMD* [54]

$$\mathcal{F}_g \equiv \int_{\mathbf{b}, \bar{\mathbf{b}}} \frac{e^{-i\mathbf{K} \cdot (\mathbf{b} - \bar{\mathbf{b}})}}{(2\pi)^4} \frac{-2}{\alpha_s} \left\langle \text{Tr} \left[ (\partial^i V_{\mathbf{b}}) V_{\bar{\mathbf{b}}}^\dagger (\partial^i V_{\bar{\mathbf{b}}}) V_{\mathbf{b}}^\dagger \right] \right\rangle_x, \quad (4)$$

represents the unintegrated gluon distribution of the target [55–57]. The argument  $x = x_{q\bar{q}}$  of the TMD is the longitudinal momentum fraction of the exchanged gluon w.r.t. the target ( $P_N^-$ ), as determined by the condition that the final  $q\bar{q}$  pair be on-shell (with  $\hat{s} \equiv 2q^+ P_N^-$ ):

$$x_{q\bar{q}} = \frac{1}{\hat{s}} \left( Q^2 + \frac{k_{1\perp}^2}{z_1} + \frac{k_{2\perp}^2}{z_2} \right) \simeq \frac{1}{\hat{s}} \left( Q^2 + \frac{P_\perp^2}{z_1 z_2} \right). \quad (5)$$

The expectation value in Eq. (4) denotes the CGC average over target fields which encodes the correlations in the gluon distribution at small  $x$ . The WW correlator depends upon  $x$  only via the high-energy evolution, as described by a special equation [58] from the BK/JIMWLK hierarchy [59–67]. For definiteness, we consider symmetric jets, with  $z_{1,2} \sim 1/2$  and  $P_\perp^2 \sim Q^2$ . But our results remain valid in the photo-production limit  $Q^2 \rightarrow 0$  so long as  $P_\perp$  is a hard scale.

If the momentum imbalance is not measured, i.e. if one integrates the cross-section Eq. (3) over  $K_\perp$  up to a value of order  $P_\perp$ , then the gluon TMD gets replaced by the gluon PDF  $xG(x, P_\perp^2)$ , which should obey the DGLAP evolution with  $P_\perp^2$ . Whereas the emergence of this evolution is well understood in the context of the collinear factorisation in the target picture, it is *a priori* less clear whether this is also encoded in the CGC framework, which follows the evolution of the projectile. A recent calculation of semi-inclusive diffractive jet production suggests that this might be indeed the case [35]. In what follows, we shall unveil the DGLAP and the CSS dynamics from a study of the NLO corrections to inclusive dijet production in the dipole picture.

To that aim, we consider (real and virtual) gluon emissions by the  $q\bar{q}$  pair. As we shall see, the emissions responsible for the DGLAP dynamics in this picture have transverse momenta  $k_{g\perp}$  in the range  $K_\perp \leq k_{g\perp} \ll P_\perp$  and longitudinal momenta  $k_g^+ = z_g q^+$  obeying  $k_{g\perp}^2/P_\perp^2 \lesssim z_g \lesssim k_{g\perp}/P_\perp \ll 1$ . The lower limit on  $z_g$  represents the boundary between the *very* soft emissions with lifetime  $\tau_g \equiv 2z_g q^+ / k_{g\perp}^2$  much shorter than the coherence time  $\tau_\gamma = 2q^+ / Q^2$  of the virtual photon, which must be included in the BK/JIMWLK evolution [68–70][71] and the *less* soft emissions ( $\tau_g \gtrsim \tau_\gamma$ ), which are relevant for the DGLAP dynamics.

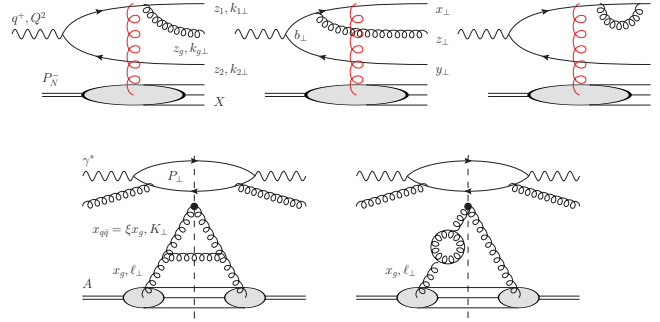


Figure 1. (Top) NLO Feynman diagrams in the dipole picture: real graphs and final state self-energy. (Bottom) Factorisation of the cross-section in the target picture.

To understand the other kinematical constraint on the gluon emissions, it is instructive to first consider the case of a *final-state* emission, which occurs long time after the collision ( $\tau_g \gg \tau_\gamma$ ). Final-state emissions of soft gluons are well known to *factorise*, thereby preserving the TMD factorisation at LO. To start with, let us consider such emissions where the gluon is both emitted and re-absorbed by the quark (see Fig. 1). To the approximations of interest, their effect on the cross-section can be seen as an additional contribution to the gluon TMD:

$$\Delta \mathcal{F}_{\text{Sud}}^{qq}(x, K_\perp^2) = \int d^2\mathbf{k}_g \int_{k_{g\perp}^2/P_\perp^2}^1 \frac{dz_g}{z_g} \frac{1}{\left(\mathbf{k}_g - \frac{z_g}{z_1} \mathbf{P}\right)^2} \times \frac{\alpha_s C_F}{\pi^2} [\mathcal{F}_g(x, \mathbf{K} + \mathbf{k}_g) - \mathcal{F}_g(x, \mathbf{K})]. \quad (6)$$

The two terms within the square brackets refer to real emissions and self-energy corrections, respectively. The denominator exhibits a collinear singularity when the relative transverse momentum of the quark-gluon pair approaches to zero. Here however we are interested in gluon emissions at large angles, outside the jet generated by the quark, which have a logarithmic phase-space: the integral over  $\mathbf{k}_g$  becomes logarithmic when  $z_g \ll k_{g\perp}/P_\perp$ . Physically, this is recognised as the condition that the gluon emission angle  $\theta_g \simeq k_{g\perp}/(z_g q^+)$  be larger than the propagation angle  $\theta_q \simeq P_\perp/q^+$  of the quark. For a given  $z_g \ll k_{g\perp}/P_\perp$ , there are two interesting ranges in  $k_{g\perp}$ : (i)  $k_{g\perp} \ll K_\perp$ . Then,  $\mathcal{F}_g(x, \mathbf{K} + \mathbf{k}_g) \simeq \mathcal{F}_g(x, \mathbf{K})$ , so the real and virtual contributions to Eq. (6) mutually cancel. (ii)  $k_{g\perp} \gg K_\perp$ . In this case,  $\mathcal{F}_g(x, \mathbf{K} + \mathbf{k}_g) \simeq \mathcal{F}_g(x, k_{g\perp}) \propto 1/k_{g\perp}^2$ , hence the real corrections are power suppressed. As for the virtual emissions, the respective integral over  $k_{g\perp}$  is logarithmic and exhibits an ultraviolet divergence, that should be removed by the standard renormalisation procedure and replaced by an upper cutoff of order  $P_\perp$ .

Thus, the net result for  $\Delta \mathcal{F}_{\text{Sud}}^{qq}$  to double-logarithmic accuracy (DLA) comes from virtual emissions with transverse momenta  $K_\perp \ll k_{g\perp} \ll P_\perp$  and longitudi-

nal fractions  $k_{g\perp}^2/P_\perp^2 \ll z_g \ll k_{g\perp}/P_\perp$ , and reads

$$\Delta\mathcal{F}_{\text{Sud}}^{qq} = -\frac{\alpha_s C_F}{\pi} \mathcal{F}_g(x, \mathbf{K}) \int_{K_\perp^2}^{P_\perp^2} \frac{dk_{g\perp}^2}{k_{g\perp}^2} \int_{\frac{k_{g\perp}^2}{P_\perp^2}}^{\frac{k_{g\perp}}{P_\perp}} \frac{dz_g}{z_g}. \quad (7)$$

Clearly, there is an identical contributions from the direct emissions by the antiquark. For such large angle emissions, one also needs to consider the interference terms, i.e. (real and virtual) final state emissions where the gluon is exchanged between the  $q\bar{q}$  pair whose leading twist contribution at large  $P_\perp$  is of order  $1/N_c$  [72]. The overall effect of the final-state gluon emissions to DLA is given by an expression similar to Eq. (7), but with the colour factor  $C_F$  replaced by  $N_c = 2C_F + 1/N_c$ :

$$\Delta\mathcal{F}_{\text{Sud}}^V(x, K_\perp^2, P_\perp^2) = -\frac{\alpha_s N_c}{4\pi} \ln^2 \frac{P_\perp^2}{K_\perp^2} \mathcal{F}_g(x, \mathbf{K}). \quad (8)$$

This is recognised as the Sudakov double logarithm for dijet production in DIS [2, 29, 73]. As shown by the notation, it also depends upon the hard resolution scale  $P_\perp$ , via the various kinematical cutoffs in Eq. (7).

Here comes our first new observation: if the imbalance  $K_\perp$  itself is relatively hard,  $Q_s \ll K_\perp \ll P_\perp$ , there is an additional double-logarithmic correction, coming from the real emissions with  $k_{g\perp} \simeq K_\perp$  — the dijet imbalance is then controlled by the gluon recoil:  $\mathbf{K} \simeq -\mathbf{k}_g$ . To see this, consider the real term in Eq. (6) in the regime where  $\ell_\perp \ll K_\perp$ , with  $\ell \equiv \mathbf{K} + \mathbf{k}_g$  the transverse momentum transferred by the target via the collision. After changing the integration variable from  $\mathbf{k}_g$  to  $\ell$  and adding the interference terms, one finds

$$\Delta\mathcal{F}_{\text{Sud}}^R = \frac{\alpha_s N_c}{\pi^2 K_\perp^2} \int_{\frac{K_\perp^2}{P_\perp^2}}^{\frac{K_\perp}{P_\perp}} \frac{dz_g}{z_g} \int_{\Lambda^2}^{K_\perp^2} d^2\ell \mathcal{F}_g(x, \ell). \quad (9)$$

The integral over  $\ell_\perp$  is recognised as the gluon PDF  $xG(x, K_\perp^2)$  (see also Eq. (20) below). This integral is logarithmic when  $\ell_\perp \gg Q_s$ , hence  $xG(x, K_\perp^2) \propto \ln(K_\perp^2/Q_s^2)$ . The virtual piece Eq. (8) dominates when  $K_\perp$  is relatively low, of order  $Q_s$ , yet both pieces behave like  $1/K_\perp^2$  when  $K_\perp \gg Q_s$ , so they contribute on the same footing when integrating over  $K_\perp$  up to  $P_\perp$ . After this integration, the real and virtual Sudakov mutually cancel, as expected on physical grounds: final-state emissions should not affect the cross-section if the dijet imbalance is not measured [2]. But this cancellation also shows that the total number of gluons  $xG(x, P_\perp^2)$  is not modified by the Sudakov dynamics. To uncover the DGLAP dynamics, one must push the NLO calculation beyond DLA.

Based on the experience with final-state emissions, we now focus on real gluon emissions with momenta  $k_{g\perp} \simeq K_\perp \gg Q_s$ , which occur either before the scattering (“initial-state”), or after it (“final-state”). As we shall see, such emissions are special in several respects: (i) they represent the leading order contributions in the double expansion in powers of  $K_\perp/P_\perp$  and

$\ell_\perp/K_\perp$ ; (ii) when expressed in terms of target longitudinal momentum variables, their contribution to the dijet cross-section factorises and can be interpreted as an additional piece  $\Delta\mathcal{F}_R$  to the gluon TMD which features the DGLAP splitting function  $P_{gg}(\xi)$  for the gluon decay  $g \rightarrow gg$ ; (iii) after adding the corresponding virtual contribution  $\Delta\mathcal{F}_V$  and integrating out the dijet imbalance  $K_\perp$ , one identifies (one step in) the DGLAP evolution of the gluon PDF  $xG(x, P_\perp^2)$ ; (iv) if  $K_\perp$  is measured too, one can construct an evolution equation for the gluon TMD, recognised as the CSS equation [11].

The starting point is an expression for the LCWF describing the  $q\bar{q}g$  fluctuation of the virtual photon in the kinematics and the approximations of interest:

$$\begin{aligned} \Psi_{\lambda_1\lambda_2}^{ija}(\mathbf{P}, \mathbf{K}, \ell, z_1, z_2) &= -i\delta_{\lambda_1\lambda_2}\delta(1-z_1-z_2)\frac{eefgq^+}{(2\pi)^6} \\ &\times \frac{\varphi^{il}(z_1, \lambda_1)}{\sqrt{z_g}} \mathcal{H}^{lm}(\mathbf{P}, z_1) \left\{ \mathcal{G}^{jmn}(\mathbf{K}, \mathcal{M}) - \frac{\delta^{mn}K^j}{K_\perp^2} \right\} \\ &\times \int d^2z e^{-i\ell \cdot z} (U_z \partial^n U_z^\dagger)^{ac} t^c. \end{aligned} \quad (10)$$

As before, we assume that  $k_{g\perp}^2/P_\perp^2 \lesssim z_g \lesssim k_{g\perp}/P_\perp$ . The additional indices  $j$  and  $a$  refer to the polarisation and the colour of the emitted gluon, while  $U_z$  denotes a Wilson line in the adjoint representation. The first term inside the braces, which features the 3rd rank tensor

$$\mathcal{G}^{jmn}(\mathbf{K}, \mathcal{M}) \equiv \frac{\partial}{\partial K^n} \frac{K^j K^m - \delta^{jm} K_\perp^2/2}{K_\perp^2 + \mathcal{M}^2}, \quad (11)$$

with  $\mathcal{M}^2 = z_g(Q^2 + P_\perp^2/(z_1 z_2))$ , corresponds to initial-state gluon emissions by either the quark or the antiquark (cf Fig. 1). After the gluon emission, the  $q\bar{q}g$  system forms an effective gluon-gluon dipole, since the transverse size  $r \sim 1/P_\perp$  of the  $q\bar{q}$  pair is much smaller than the separation  $R \equiv |\mathbf{z} - \mathbf{b}| \sim 1/K_\perp$  between this pair located at  $\mathbf{b}$  and the gluon at  $\mathbf{z}$ . The traceless 2nd rank tensor with indices ( $jm$ ) is the hallmark of this  $gg$  dipole [34, 74–77]. Its collision with the nucleus is described by a colour operator similar to that at LO,

$$\begin{aligned} U_z^{ac} V_x t^c V_y^\dagger - t^a &\simeq U_z^{ac} V_b t^c V_b^\dagger - t^a = (U_z U_b^\dagger)^{ac} t^c - t^a \\ &\simeq -R^n (U_z \partial^n U_z^\dagger)^{ac} t^c. \end{aligned} \quad (12)$$

The final expansion is legitimate as the size  $R$  of the  $gg$  dipole is small compared to the typical scale  $1/\ell_\perp \sim 1/Q_s$  for variations in the target field. After Fourier transform from  $\mathbf{R}$  to  $\mathbf{K}$ , the factor  $R^n$  in Eq. (12) yields the derivative w.r.t.  $K^n$  in Eq. (11). The second term inside the braces in Eq. (10) refers to final state emissions already computed in Eq. (9) at the cross-section level. After the gluon emission, the WW gluon TMD appears again in the cross-section, but at the lower scale  $\ell_\perp$ .

Although Eq. (10) involves the same hard factor as the LO amplitude Eq. (1), the TMD factorisation is not yet

manifest: indeed, the tensor Eq. (11) depends upon both  $K_\perp$  and the kinematical variables of the hard  $q\bar{q}$  pair, via the quantity  $\mathcal{M}^2$ . In this case, TMD factorisation would mean that the gluon can be re-interpreted as a component of the target wavefunction. As shown in [34, 35], this is indeed possible for a soft gluon ( $z_g \ll K_\perp/P_\perp$ ): it amounts to a change of longitudinal variables. We first observe that, in order for the final  $q\bar{q}g$  system to be on-shell, the target must transfer via the collision a “minus” longitudinal momentum  $x_g P_N^-$  with (compare to Eq. (5))

$$x_g = \frac{1}{\hat{s}} \left( \frac{k_{1\perp}^2}{z_1} + \frac{k_{2\perp}^2}{z_2} + \frac{k_{g\perp}^2}{z_g} + Q^2 \right) \simeq \frac{\mathcal{M}^2 + K_\perp^2}{z_g \hat{s}}. \quad (13)$$

A fraction  $\xi = x_{q\bar{q}}/x_g$  of this momentum must be taken by the hard  $q\bar{q}$  pair, while the remaining fraction  $1 - \xi$  goes to the gluon. The condition that the gluon be on-shell,  $2z_g(1 - \xi)x_g q^+ P_N^- = K_\perp^2$ , together with Eq. (13) fixes the relation between  $\xi$  and  $z_g$ :

$$z_g = \frac{\xi}{1 - \xi} \frac{K_\perp^2}{Q^2 + P_\perp^2/(z_1 z_2)}, \quad (14)$$

After this change of variables,  $\mathcal{M}^2 = \frac{\xi}{1 - \xi} K_\perp^2$  can be expressed in terms of target variables only. Together with Eq. (10), this leads to an expression for the hard dijet cross-section where TMD factorisation becomes manifest. This is similar to Eq. (3), but with the LO gluon TMD  $\mathcal{F}_g^{(0)}$  replaced by the following NLO contribution:

$$\Delta\mathcal{F}_R = \frac{\alpha_s}{2\pi K_\perp^2} \int_{x_*}^{1 - \xi_0(K_\perp)} d\xi P_{gg}(\xi) \int_{\Lambda^2}^{K_\perp^2} d\ell_\perp^2 \mathcal{F}_g^{(0)} \left( \frac{x}{\xi}, \ell_\perp^2 \right). \quad (15)$$

It is understood that  $x \equiv x_{q\bar{q}}$ , hence the argument  $x/\xi$  of the LO gluon TMD under the integral takes the correct value  $x_g$ . As anticipated, Eq. (15) involves the (unregularised)  $g \rightarrow gg$  splitting function

$$P_{gg}(\xi) = 2N_c \frac{1 + (1 - \xi)^2(1 + \xi^2) - (1 - \xi^2)}{\xi(1 - \xi)}. \quad (16)$$

The three pieces in the decomposition of the numerator correspond to emissions in the final state, in the initial state, and to interferences between the two, respectively, see Fig. 1. (The singular piece  $2N_c/[\xi(1 - \xi)]$  has been exclusively generated via final-state emissions, cf. Eq. (9).)

The integration limits on  $\xi$  in Eq. (15) follow from the corresponding limits on  $z_g$  in Eq. (9) together with Eq. (14): (a) The condition  $z_g \ll k_{g\perp}/P_\perp$  together with  $k_{g\perp} \simeq K_\perp$  implies  $\xi \ll 1 - \xi_0(K_\perp)$  with  $\xi_0(K_\perp) \equiv K_\perp/P_\perp \ll 1$ . This upper limit is only important for the piece of  $P_{gg}(\xi)$  which is singular at  $\xi \rightarrow 1$ ; for the other pieces, one can safely let  $\xi_0 \rightarrow 0$ , since the respective dependence upon  $\xi_0$  is power-suppressed. (b) The lower limit on  $z_g$  in Eq. (9), which we recall marks the

separation from the high-energy evolution, will be more precisely written as  $z_g \geq x_*(k_{g\perp}^2/P_\perp^2)$ , with  $x_* \ll 1$  and such that  $\alpha_s \ln(1/x_*) \ll 1$ . Together with Eq. (14), this implies  $\xi \gtrsim x_*$ . Changing the value of  $x_*$  should be seen as a form of scheme dependence [78]. For latter convenience, it is useful to isolate the  $\xi_0$  dependence from the integral over  $\xi$  with the help of the plus prescription:

$$\begin{aligned} \Delta\mathcal{F}_R &= \frac{\alpha_s}{2\pi K_\perp^2} \int_{x_*}^1 d\xi P_{gg}^{(+)}(\xi) \int_{\Lambda^2}^{K_\perp^2} d\ell_\perp^2 \mathcal{F}_g^{(0)} \left( \frac{x}{\xi}, \ell_\perp^2 \right) \\ &+ \frac{\alpha_s N_c}{2\pi K_\perp^2} \ln \frac{P_\perp^2}{K_\perp^2} \int_{\Lambda^2}^{K_\perp^2} d\ell_\perp^2 \mathcal{F}_g^{(0)}(x, \ell_\perp^2), \end{aligned} \quad (17)$$

where  $P_{gg}^{(+)}$  differs from Eq. (16) only in the replacement  $(1 - \xi) \rightarrow (1 - \xi)_+$  in the denominator. The second term is recognised as the real Sudakov contribution Eq. (9).

Although obtained via a NLO calculation in the dipole picture, the result Eq. (17) can naturally be interpreted in the target picture, as a (real) gluon emission by the gluon exchanged in the  $t$ -channel (see Fig. 1). This is similar to one step in the DGLAP evolution: a gluon with some initial transverse momentum  $\ell_\perp \ll K_\perp$  undergoes a hard splitting, giving rise to a pair of gluons with momenta  $\pm K$ . But unlike in the standard DGLAP set-up, the final momentum  $K_\perp$  is also measured, so one evolves the TMD.

A complete evolution also requires the corresponding virtual corrections — those associated with gluon emissions within the range  $K_\perp \ll k_{g\perp} \ll P_\perp$ ,

$$\begin{aligned} \Delta\mathcal{F}_V &= -\frac{\alpha_s}{4\pi} \int_{K_\perp^2}^{P_\perp^2} \frac{d\ell_\perp^2}{\ell_\perp^2} \int_{\xi_0(\ell_\perp)}^{1 - \xi_0(\ell_\perp)} d\xi P_{gg}(\xi) \mathcal{F}_g^{(0)}(x, K_\perp^2) \\ &\simeq -\frac{\alpha_s N_c}{\pi} \left( \frac{1}{4} \ln^2 \frac{P_\perp^2}{K_\perp^2} - \beta_0 \ln \frac{P_\perp^2}{K_\perp^2} \right) \mathcal{F}_g^{(0)}(x, K_\perp^2), \end{aligned} \quad (18)$$

where  $\beta_0 = 11/12$ . The double-logarithmic term in the second line has been generated by the singular piece  $2N_c/[\xi(1 - \xi)]$  of the splitting function; it coincides with our previous result Eq. (8), as it should. The  $\beta_0$ -piece is not naturally generated by the NLO calculation in the dipole picture [29–31], because of the classical approximation used for the scattering with the target [6, 7]. In the target picture, this piece arises from the gluon self-energy insertion into the propagator of the exchanged gluon (see Fig. 1). It corresponds to running coupling corrections to the gluon TMD Eq. (4) [79, 80], to be simultaneously considered with the respective corrections to the coupling appearing in Eq. (3) [30]. In what follows, we shall keep this piece in  $\Delta\mathcal{F}_V$  (as we shall see, it is needed in order to get the full DGLAP equation) and, for consistency, replace  $\alpha_s \rightarrow \alpha_s(P_\perp^2)$  in Eq. (3).

The one-loop approximation  $\mathcal{F}_g = \mathcal{F}_g^{(0)} + \Delta\mathcal{F}_R + \Delta\mathcal{F}_V$  can be now promoted into an evolution equation for the gluon TMD with increasing  $P_\perp$ . To that aim, we first

take the derivative of  $\mathcal{F}_g$  w.r.t.  $\ln P_\perp^2$  and then insert the resolution scale  $P_\perp^2$  in the gluon TMDs from the r.h.s. by

$$\begin{aligned} \frac{\partial \mathcal{F}_g(x, K_\perp^2, P_\perp^2)}{\partial \ln P_\perp^2} = & \frac{N_c}{2\pi} \left\{ \frac{\alpha_s(K_\perp^2)}{K_\perp^2} \int_{\Lambda^2}^{K_\perp^2} d\ell_\perp^2 \mathcal{F}_g(x, \ell_\perp^2, P_\perp^2) - \int_{K_\perp^2}^{P_\perp^2} \frac{d\ell_\perp^2}{\ell_\perp^2} \alpha_s(\ell_\perp^2) \mathcal{F}_g(x, K_\perp^2, P_\perp^2) \right\} \\ & + \beta_0 \frac{\alpha_s(P_\perp^2) N_c}{\pi} \mathcal{F}_g(x, K_\perp^2, P_\perp^2). \end{aligned} \quad (19)$$

In all the terms,  $\alpha_s$  runs with the transverse momentum of the daughter gluons produced by the hard splitting.

Eq. (19) can be recognised as the momentum-space version of the CSS equation [81–86][87]. It is related via a Fourier transform to the coordinate-space version commonly used in the literature [88–90]. Although the  $\mathbf{b}_\perp$ -space formulation allows for a smoother matching onto the non-perturbative [11, 12] or saturation [1, 2] regimes, the momentum-space version makes the transverse-momentum dynamics more transparent: Eq. (19) is a *rate equation*, with a “gain term” and a “loss term” (the first and second terms in the r.h.s., respectively), which describes the change in the  $K_\perp$ -distribution when increasing the resolution scale  $P_\perp^2$ . Increasing  $P_\perp$  reduces the longitudinal cutoff  $\xi_0$  and hence opens up the phase-space for additional gluon emissions with longitudinal fractions  $1 - \xi \ll 1$ . Via such an emission, the number of gluons in the bin at  $K_\perp$  can either increase (via the process  $\ell_\perp \rightarrow (\mathbf{K}, -\mathbf{K})$  where  $\ell_\perp \ll K_\perp$ ), or decrease (via the process  $\mathbf{K} \rightarrow (\mathbf{K}', -\mathbf{K}')$  where  $K_\perp \ll K'_\perp \ll P_\perp$ ). Since  $\xi \simeq 1$  for any of these soft splittings, the CSS evolution is local in  $x$ . We thus see that the CSS dynamics redistributes the (measured) gluons in  $K_\perp$  without affecting their longitudinal momentum, nor their total number: indeed, if one integrates the r.h.s. of Eq. (19) over  $K_\perp^2$  up to  $P_\perp^2$ , then the first two terms precisely cancel each other. The term proportional to  $\beta_0$  merely accounts for running coupling corrections and allows to reconstruct the full DGLAP splitting function.

To that aim, we use the relation between the TMD and the PDF in the presence of scale dependence [91]:

$$xG(x, Q^2) = \pi \int_{\Lambda^2}^{Q^2} dK_\perp^2 \mathcal{F}_g(x, K_\perp^2, Q^2). \quad (20)$$

Its derivative w.r.t.  $Q^2$  involves two terms, one coming from the upper limit of the integral — the boundary value  $\mathcal{F}_g(x, Q^2, Q^2)$  determined by the first line of Eq. (17) with  $\mathcal{F}_g^{(0)} \rightarrow \mathcal{F}_g$  — and another coming from the  $Q^2$  dependence of the TMD. As just mentioned, the second term receives a non-zero contribution only from the  $\beta_0$ -piece of Eq. (19). This contribution adds to  $P_{gg}^{(+)}$  in Eq. (17), thus completing the standard expression for

requiring this evolution to be a Markovian process — the r.h.s. must be *local in  $P_\perp^2$* . One thus finds

the regularised DGLAP splitting function  $\mathcal{P}_{gg}$  [11]. We thus deduce the evolution equation for the gluon PDF

$$\begin{aligned} \frac{\partial xG(x, Q^2)}{\partial \ln Q^2} = & \pi Q^2 \mathcal{F}^{(0)}(x, Q^2) \\ & + \frac{\alpha_s(Q^2)}{2\pi} \int_{x_*}^1 d\xi \mathcal{P}_{gg}(\xi) \frac{x}{\xi} G\left(\frac{x}{\xi}, Q^2\right), \end{aligned} \quad (21)$$

which is the expected DGLAP equation, but supplemented with a source term and with a lower limit  $x_*$  (instead of the standard value  $x$ ) on the integral over  $\xi$ . These special features reflect the fact that Eq. (21) holds in the context of small- $x$  factorisation: the DGLAP evolution applies on top of the high-energy evolution.

To summarise, the DGLAP+CSS evolution of the gluon TMD is encoded in the solution to Eq. (19) with the following initial condition at  $P_\perp^2 = K_\perp^2$ :

$$\begin{aligned} \mathcal{F}_g(x, K_\perp^2, K_\perp^2) = & \frac{1}{\pi} \frac{\partial xG(x, K_\perp^2)}{\partial K_\perp^2} \\ & - \frac{\beta_0 N_c}{\pi^2} \frac{\alpha_s(K_\perp^2)}{K_\perp^2} xG(x, K_\perp^2), \end{aligned} \quad (22)$$

where the derivative term is defined by Eq. (21). Eq. (22) describes the change in the number of gluons with momentum  $K_\perp$  due to the DGLAP evolution up to  $K_\perp^2$ , while the CSS equation describes the respective change due to the increase in the resolution scale  $P_\perp^2$ .

The phase-space for this DGLAP evolution starts at transverse momenta, or virtualities, of order  $Q_s(x)$ . If  $P_\perp \gg K_\perp \gg Q_s$ , as is generally the case for dijet production in ultraperipheral nucleus-nucleus collisions at the LHC [92, 93], then both types of evolution, DGLAP and CSS, must be taken into account. Besides, since  $x \equiv x_{q\bar{q}} \ll 1$ , the high-energy BK/JIMWLK evolution is important as well. In practice, one should proceed as follows (see Fig. 2): (i) one should first compute the gluon WW TMD from numerical solutions to the JIMWLK equation for all the values of  $x$  and  $K_\perp$  of interest, starting with some convenient initial condition at  $x_0 \sim 10^{-2}$ , like the MV model [55, 56]; this step will provide the LO result  $\mathcal{F}_g^{(0)}(x, K_\perp)$ ; (ii) using this LO result as a source term, one should next solve the DGLAP

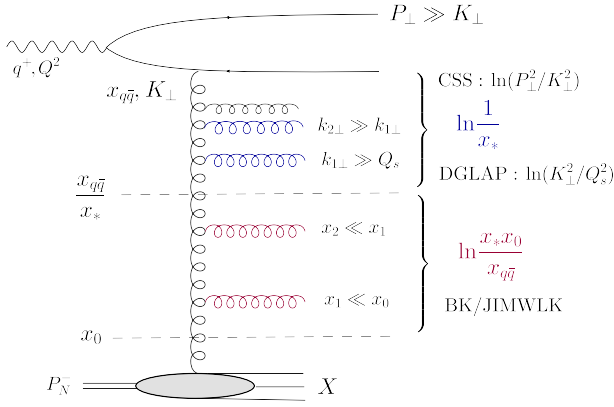


Figure 2. Diagram of the three types of evolution which matter for dijet production at small  $x$  and for  $P_\perp \gg K_\perp \gg Q_s$ .

equation Eq. (21); there is some overlap in rapidity, at  $x_* < \xi < 1$ , between the longitudinal phase-spaces for the JIMWLK and respectively the DGLAP evolutions, but so long as  $\alpha_s \ln(1/x_*) \ll 1$ , this is a pure-NLO effect; (iii) the solution  $xG(x, K_\perp^2)$  to the DGLAP equation should be used as an initial condition for the CSS evolution Eq. (19) up to  $P_\perp^2$ . To our knowledge, it is the first time such a procedure is shown to emerge from a first principle calculation at small  $x$ .

Similar results can be obtained for other processes, like  $\gamma$ -jet production in  $pA$  collisions (which involves the dipole gluon TMD) and semi-inclusive jet production in DIS, which features the quark (inclusive or diffractive) TMD. They will be presented in separate publications.

**Acknowledgements.** We are grateful to Al Mueller and Feng Yuan for inspiring discussions. We would like to thank Sigtryggur Hauksson and Farid Salazar for useful remarks. The figures were created with JaxoDraw [94].

\* caucal@subatech.in2p3.fr

† edmond.iancu@ipht.fr

- [1] A. H. Mueller, B.-W. Xiao, and F. Yuan, *Phys. Rev. Lett.* **110**, 082301 (2013), arXiv:1210.5792 [hep-ph].
- [2] A. Mueller, B.-W. Xiao, and F. Yuan, *Phys. Rev. D* **88**, 114010 (2013), arXiv:1308.2993 [hep-ph].
- [3] I. Balitsky and A. Tarasov, *JHEP* **10**, 017 (2015), arXiv:1505.02151 [hep-ph].
- [4] I. Balitsky and A. Tarasov, *JHEP* **06**, 164 (2016), arXiv:1603.06548 [hep-ph].
- [5] J. Zhou, *JHEP* **06**, 151 (2016), arXiv:1603.07426 [hep-ph].
- [6] B.-W. Xiao, F. Yuan, and J. Zhou, *Nucl. Phys. B* **921**, 104 (2017), arXiv:1703.06163 [hep-ph].
- [7] M. Hentschinski, *Phys. Rev. D* **104**, 054014 (2021), arXiv:2107.06203 [hep-ph].
- [8] R. Boussarie and Y. Mehtar-Tani, *JHEP* **07**, 080 (2022), arXiv:2112.01412 [hep-ph].
- [9] Y. Fu, Z.-B. Kang, F. Salazar, X.-N. Wang, and H. Xing, (2023), arXiv:2310.12847 [hep-ph].

- [10] S. Mukherjee, V. V. Skokov, A. Tarasov, and S. Tiwari, *Phys. Rev. D* **109**, 034035 (2024), arXiv:2311.16402 [hep-ph].
- [11] J. Collins, *Foundations of Perturbative QCD*, Cambridge Monographs on Particle Physics, Nuclear Physics and Cosmology, Vol. 32 (Cambridge University Press, 2023).
- [12] R. Boussarie *et al.*, (2023), arXiv:2304.03302 [hep-ph].
- [13] F. Dominguez, B.-W. Xiao, and F. Yuan, *Phys. Rev. Lett.* **106**, 022301 (2011), arXiv:1009.2141 [hep-ph].
- [14] F. Dominguez, C. Marquet, B.-W. Xiao, and F. Yuan, *Phys. Rev. D* **83**, 105005 (2011), arXiv:1101.0715 [hep-ph].
- [15] A. Metz and J. Zhou, *Phys. Rev. D* **84**, 051503 (2011), arXiv:1105.1991 [hep-ph].
- [16] F. Dominguez, J.-W. Qiu, B.-W. Xiao, and F. Yuan, *Phys. Rev. D* **85**, 045003 (2012), arXiv:1109.6293 [hep-ph].
- [17] A. Dumitru, T. Lappi, and V. Skokov, *Phys. Rev. Lett.* **115**, 252301 (2015), arXiv:1508.04438 [hep-ph].
- [18] P. Kotko, K. Kutak, C. Marquet, E. Petreska, S. Sapeta, and A. van Hameren, *JHEP* **09**, 106 (2015), arXiv:1503.03421 [hep-ph].
- [19] C. Marquet, E. Petreska, and C. Roiesnel, *JHEP* **10**, 065 (2016), arXiv:1608.02577 [hep-ph].
- [20] A. van Hameren, P. Kotko, K. Kutak, C. Marquet, E. Petreska, and S. Sapeta, *JHEP* **12**, 034 (2016), arXiv:1607.03121 [hep-ph].
- [21] C. Marquet, C. Roiesnel, and P. Tael, *Phys. Rev. D* **97**, 014004 (2018), arXiv:1710.05698 [hep-ph].
- [22] J. L. Albacete, G. Giacalone, C. Marquet, and M. Matas, *Phys. Rev. D* **99**, 014002 (2019), arXiv:1805.05711 [hep-ph].
- [23] A. Dumitru, V. Skokov, and T. Ullrich, *Phys. Rev. C* **99**, 015204 (2019), arXiv:1809.02615 [hep-ph].
- [24] R. Boussarie, H. Mäntysaari, F. Salazar, and B. Schenke, *JHEP* **09**, 178 (2021), arXiv:2106.11301 [hep-ph].
- [25] P. Kotko, K. Kutak, S. Sapeta, A. M. Stasto, and M. Strikman, *Eur. Phys. J. C* **77**, 353 (2017), arXiv:1702.03063 [hep-ph].
- [26] K. Roy and R. Venugopalan, *Phys. Rev. D* **101**, 034028 (2020), arXiv:1911.04530 [hep-ph].
- [27] K. Roy and R. Venugopalan, *Phys. Rev. D* **101**, 071505 (2020), arXiv:1911.04519 [hep-ph].
- [28] P. Caucal, F. Salazar, and R. Venugopalan, *JHEP* **11**, 222 (2021), arXiv:2108.06347 [hep-ph].
- [29] P. Tael, T. Altinoluk, G. Beuf, and C. Marquet, *JHEP* **10**, 184 (2022), arXiv:2204.11650 [hep-ph].
- [30] P. Caucal, F. Salazar, B. Schenke, T. Stebel, and R. Venugopalan, *JHEP* **08**, 062 (2023), arXiv:2304.03304 [hep-ph].
- [31] P. Caucal, F. Salazar, B. Schenke, T. Stebel, and R. Venugopalan, *Phys. Rev. Lett.* **132**, 081902 (2024), arXiv:2308.00022 [hep-ph].
- [32] E. Iancu, A. H. Mueller, and D. N. Triantafyllopoulos, *Phys. Rev. Lett.* **128**, 202001 (2022), arXiv:2112.06353 [hep-ph].
- [33] Y. Hatta, B.-W. Xiao, and F. Yuan, *Phys. Rev. D* **106**, 094015 (2022), arXiv:2205.08060 [hep-ph].
- [34] E. Iancu, A. H. Mueller, D. N. Triantafyllopoulos, and S. Y. Wei, *JHEP* **10**, 103 (2022), arXiv:2207.06268 [hep-ph].
- [35] S. Hauksson, E. Iancu, A. H. Mueller, D. N. Triantafyllopoulos, and S. Y. Wei, (2024), arXiv:2402.14748 [hep-ph].
- [36] E. Iancu, A. Leonidov, and L. McLerran, in *Cargese Summer School on QCD Perspectives on Hot and Dense Matter* (2002) pp. 73–145, arXiv:hep-ph/0202270.
- [37] E. Iancu and R. Venugopalan, “The Color glass conden-

- sate and high-energy scattering in QCD," in *Quark-gluon plasma 4*, edited by R. C. Hwa and X.-N. Wang (2003) pp. 249–3363, [arXiv:hep-ph/0303204](#).
- [38] F. Gelis, E. Iancu, J. Jalilian-Marian, and R. Venugopalan, *Ann. Rev. Nucl. Part. Sci.* **60**, 463 (2010), [arXiv:1002.0333 \[hep-ph\]](#).
- [39] Y. V. Kovchegov and E. Levin, *Quantum Chromodynamics at High Energy*, Vol. 33 (Oxford University Press, 2013).
- [40] V. Gribov and L. Lipatov, *Sov.J.Nucl.Phys.* **15**, 438 (1972).
- [41] G. Altarelli and G. Parisi, *Nucl.Phys.* **B126**, 298 (1977).
- [42] Y. L. Dokshitzer, *Sov.Phys.JETP* **46**, 641 (1977).
- [43] J. C. Collins and D. E. Soper, *Nucl. Phys. B* **193**, 381 (1981), [Erratum: *Nucl.Phys.B* 213, 545 (1983)].
- [44] J. C. Collins and D. E. Soper, *Nucl. Phys. B* **194**, 445 (1982).
- [45] J. C. Collins, D. E. Soper, and G. F. Sterman, *Nucl. Phys. B* **250**, 199 (1985).
- [46] We work in a frame where the photon with virtuality  $Q^2$  is an ultrarelativistic right-mover, with longitudinal momentum  $q^+ \gg \sqrt{Q^2}$ , while the nucleus is a left-mover with longitudinal momentum  $P_N^-$  per nucleon.
- [47] B. Z. Kopeliovich, L. I. Lapidus, and A. B. Zamolodchikov, *JETP Lett.* **33**, 595 (1981).
- [48] G. Bertsch, S. J. Brodsky, A. S. Goldhaber, and J. F. Gunion, *Phys. Rev. Lett.* **47**, 297 (1981).
- [49] A. H. Mueller, *Nucl.Phys.* **B335**, 115 (1990).
- [50] N. N. Nikolaev and B. Zakharov, *Z.Phys.* **C49**, 607 (1991).
- [51] L. Zheng, E. Aschenauer, J. Lee, and B.-W. Xiao, *Phys. Rev. D* **89**, 074037 (2014), [arXiv:1403.2413 \[hep-ph\]](#).
- [52] Y.-Y. Zhao, M.-M. Xu, L.-Z. Chen, D.-H. Zhang, and Y.-F. Wu, *Phys. Rev. D* **104**, 114032 (2021), [arXiv:2105.08818 \[hep-ph\]](#).
- [53] E. Iancu and Y. Mulian, *JHEP* **07**, 121 (2023), [arXiv:2211.04837 \[hep-ph\]](#).
- [54] We only consider here the unpolarized WW gluon TMD. A similar study of the linearly polarized WW TMD [15] will be presented in a companion paper.
- [55] L. D. McLerran and R. Venugopalan, *Phys. Rev. D* **49**, 3352 (1994), [arXiv:hep-ph/9311205](#).
- [56] L. D. McLerran and R. Venugopalan, *Phys. Rev. D* **49**, 2233 (1994), [arXiv:hep-ph/9309289](#).
- [57] L. D. McLerran and R. Venugopalan, *Phys. Rev. D* **59**, 094002 (1999), [arXiv:hep-ph/9809427](#).
- [58] F. Dominguez, A. H. Mueller, S. Munier, and B.-W. Xiao, *Phys. Lett. B* **705**, 106 (2011), [arXiv:1108.1752 \[hep-ph\]](#).
- [59] I. Balitsky, *Nucl. Phys. B* **463**, 99 (1996), [arXiv:hep-ph/9509348](#).
- [60] Y. V. Kovchegov, *Phys. Rev. D* **60**, 034008 (1999), [arXiv:hep-ph/9901281](#).
- [61] J. Jalilian-Marian, A. Kovner, A. Leonidov, and H. Weigert, *Nucl. Phys. B* **504**, 415 (1997), [arXiv:hep-ph/9701284](#).
- [62] J. Jalilian-Marian, A. Kovner, A. Leonidov, and H. Weigert, *Phys.Rev.* **D59**, 014014 (1998), [arXiv:hep-ph/9706377 \[hep-ph\]](#).
- [63] A. Kovner, J. G. Milhano, and H. Weigert, *Phys. Rev. D* **62**, 114005 (2000), [arXiv:hep-ph/0004014](#).
- [64] H. Weigert, *Nucl. Phys. A* **703**, 823 (2002), [arXiv:hep-ph/0004044](#).
- [65] E. Iancu, A. Leonidov, and L. D. McLerran, *Nucl. Phys. A* **692**, 583 (2001), [arXiv:hep-ph/0011241](#).
- [66] E. Iancu, A. Leonidov, and L. D. McLerran, *Phys. Lett. B* **510**, 133 (2001), [arXiv:hep-ph/0102009](#).
- [67] E. Ferreiro, E. Iancu, A. Leonidov, and L. McLerran, *Nucl. Phys. A* **703**, 489 (2002), [arXiv:hep-ph/0109115](#).
- [68] G. Beuf, *Phys.Rev.* **D89**, 074039 (2014), [arXiv:1401.0313 \[hep-ph\]](#).
- [69] E. Iancu, J. Madrigal, A. Mueller, G. Soyez, and D. Triantafyllopoulos, *Phys.Lett. B* **744**, 293 (2015), [arXiv:1502.05642 \[hep-ph\]](#).
- [70] B. Ducloué, E. Iancu, A. H. Mueller, G. Soyez, and D. N. Triantafyllopoulos, *JHEP* **04**, 081 (2019), [arXiv:1902.06637 \[hep-ph\]](#).
- [71] The constraint  $\tau_g \ll \tau_\gamma$  or, equivalently,  $z_g \ll k_{g\perp}^2/Q^2$ , is at the origin of the collinear improvement of the BK/BFKL equation, which achieves an all-order resummation of radiative corrections enhanced by transverse double logarithms [68, 69, 95–103].
- [72] The would-be dominant contribution of the interference terms in the multicolour limit  $N_c \rightarrow \infty$  is non-zero, but it describes double scattering — it is proportional to the square of the dipole scattering amplitude —, so in the high  $P_\perp$  regime of interest, it is strongly suppressed by the colour transparency of small dipoles.
- [73] P. Caucal, F. Salazar, B. Schenke, and R. Venugopalan, *JHEP* **11**, 169 (2022), [arXiv:2208.13872 \[hep-ph\]](#).
- [74] M. Wusthoff, *Phys. Rev. D* **56**, 4311 (1997), [arXiv:hep-ph/9702201](#).
- [75] K. J. Golec-Biernat and M. Wusthoff, *Phys. Rev. D* **60**, 114023 (1999), [arXiv:hep-ph/9903358](#).
- [76] A. Hebecker, *Nucl. Phys. B* **505**, 349 (1997), [arXiv:hep-ph/9702373](#).
- [77] W. Buchmuller, T. Gehrmann, and A. Hebecker, *Nucl. Phys. B* **537**, 477 (1999), [arXiv:hep-ph/9808454](#).
- [78] In a full NLO calculation, the dependence upon  $x_*$  should cancel among the NLO contributions to the JIMWLK and DGLAP evolutions and to the hard factor. Beyond a fixed order, the double-logarithmic corrections proportional to powers of  $\alpha_s \ln(1/x_*) \ln(K_\perp^2/\Lambda^2)$  should cancel between the results of the JIMWLK and the DGLAP evolutions.
- [79] A. Ayala, J. Jalilian-Marian, L. D. McLerran, and R. Venugopalan, *Phys. Rev. D* **53**, 458 (1996), [arXiv:hep-ph/9508302](#).
- [80] J. Zhou, *Phys. Rev. D* **99**, 054026 (2019), [arXiv:1807.00506 \[hep-ph\]](#).
- [81] Y. L. Dokshitzer, D. Diakonov, and S. I. Troian, *Phys. Rept.* **58**, 269 (1980).
- [82] Y. L. Dokshitzer, D. Diakonov, and S. I. Troian, *Phys. Lett. B* **79**, 269 (1978).
- [83] R. K. Ellis and S. Veseli, *Nucl. Phys. B* **511**, 649 (1998), [arXiv:hep-ph/9706526](#).
- [84] S. Frixione, P. Nason, and G. Ridolfi, *Nucl. Phys. B* **542**, 311 (1999), [arXiv:hep-ph/9809367](#).
- [85] P. F. Monni, E. Re, and P. Torrielli, *Phys. Rev. Lett.* **116**, 242001 (2016), [arXiv:1604.02191 \[hep-ph\]](#).
- [86] M. A. Ebert and F. J. Tackmann, *JHEP* **02**, 110 (2017), [arXiv:1611.08610 \[hep-ph\]](#).
- [87] In general, the evolution variable in the CSS equation is the rapidity cutoff  $\ln(1/\xi_0)$ . In the present context though, where  $\xi_0 = K_\perp/P_\perp$ , this becomes a transverse logarithm.
- [88] A. Kulesza and W. J. Stirling, *Nucl. Phys. B* **555**, 279 (1999), [arXiv:hep-ph/9902234](#).
- [89] A. Kulesza and W. J. Stirling, *JHEP* **01**, 016 (2000), [arXiv:hep-ph/9909271](#).
- [90] A. Kulesza and W. J. Stirling, *Eur. Phys. J. C* **20**, 349

- (2001), [arXiv:hep-ph/0103089](#).
- [91] M. A. Ebert, J. K. L. Michel, I. W. Stewart, and Z. Sun, *JHEP* **07**, 129 (2022), [arXiv:2201.07237 \[hep-ph\]](#).
- [92] ATLAS-CONF-2022-021 (2022).
- [93] A. Tumasyan *et al.* (CMS), *Phys. Rev. Lett.* **131**, 051901 (2023), [arXiv:2205.00045 \[nucl-ex\]](#).
- [94] D. Binosi and L. Theussl, *Comput.Phys.Commun.* **161**, 76 (2004), [arXiv:hep-ph/0309015 \[hep-ph\]](#).
- [95] B. Andersson, G. Gustafson, and J. Samuelsson, *Nucl.Phys.* **B467**, 443 (1996).
- [96] J. Kwiecinski, A. D. Martin, and P. J. Sutton, *Z. Phys.* **C71**, 585 (1996), [arXiv:hep-ph/9602320 \[hep-ph\]](#).
- [97] J. Kwiecinski, A. D. Martin, and A. Stasto, *Phys.Rev.* **D56**, 3991 (1997), [arXiv:hep-ph/9703445 \[hep-ph\]](#).
- [98] G. Salam, *JHEP* **9807**, 019 (1998), [arXiv:hep-ph/9806482 \[hep-ph\]](#).
- [99] M. Ciafaloni and D. Colferai, *Phys.Lett.* **B452**, 372 (1999), [arXiv:hep-ph/9812366 \[hep-ph\]](#).
- [100] M. Ciafaloni, D. Colferai, and G. Salam, *Phys.Rev.* **D60**, 114036 (1999), [arXiv:hep-ph/9905566 \[hep-ph\]](#).
- [101] M. Ciafaloni, D. Colferai, G. Salam, and A. Stasto, *Phys.Rev.* **D68**, 114003 (2003), [arXiv:hep-ph/0307188 \[hep-ph\]](#).
- [102] A. Sabio Vera, *Nucl. Phys. B* **722**, 65 (2005), [arXiv:hep-ph/0505128](#).
- [103] L. Motyka and A. M. Stasto, *Phys.Rev.* **D79**, 085016 (2009), [arXiv:0901.4949 \[hep-ph\]](#).